A time series analysis of transparent exopolymer particle distributions and C:N stoichiometry in the subtropical North Pacific: a key process in net community production and preformed nitrate anomalies?

Kieran Curran[1], Tracy A. Villareal[2], Robert T. Letscher[1,3]

1 Ocean Process Analysis Laboratory, University of New Hampshire, Durham, NH, 03824 USA
2 Marine Science Institute, University of Texas at Austin, Port Aransas, TX 78373 USA
3 Department of Earth Sciences, University of New Hampshire, Durham, NH 03824 USA

Correspondence to: Robert T. Letscher (robert.letscher@unh.edu)

Abstract

Within the oligotrophic subtropical oceans, summertime dissolved inorganic carbon drawdown despite nutrient limitation in surface waters and subsurface oxygen consumption in the absence of Redfieldian stoichiometric nitrate release are two phenomena still awaiting a full mechanistic characterization. Many processes may contribute to these anomalies including N_2 fixation, non-Redfieldian DOM cycling, vertically migrating phytoplankton, heterotrophic NO_3^- uptake and vertical NO_3^- injection events. While these processes have been measured or modelled they generally cannot fully account for the magnitudes of oxygen/nitrate anomalies and excess dissolved inorganic drawdown observed in many oligotrophic subtropical waters. One other candidate process that may contribute to both phenomena is the formation of carbon-rich transparent exopolymer particles (TEP) and Coomassie-stainable particles (CSP) from dissolved organic precursors in surface waters and their subsequent export and remineralization below, however, few TEP and CSP data exist from the oligotrophic ocean. Here we present a multi-year time-series (Jan 2020 – Sep 2022) analysis of TEP, CSP and total dissolved carbohydrate concentrations at both Station ALOHA (22˚45',158 ˚W) and along a meridional transect during June 2021 from 22˚45' to 31˚N within the North Pacific subtropical gyre. Exopolymer C:N stoichiometry at Station ALOHA varied between 16.4 – 34.3, with values being more carbon-rich in summer (26-34); ratios were higher (33-38) toward the gyre centre at 31˚N. TEP concentrations were consistently elevated in surface waters through Spring-Autumn (4-8 µM C after carbon conversion) at Station ALOHA with lower concentrations (~1.5-3 µM C) and more uniform vertical distribution during winter, indicating that TEP accumulated in surface waters may vertically sink and be exported with winter mixing. The accumulation of exopolymers in surface waters through Spring-Autumn and its subsequent vertical export may account for 6.5-20% of net community production, helping to reduce the estimated imbalance of N supply and demand at this site to <10%. The upper ocean exopolymer cycle may explain 22-67% of the observed oxygen/nitrate anomalies, helping to close the C, N, and O_2 budgets at station ALOHA, while leaving room for significant contributions from other processes such as vertically migrating phytoplankton and heterotrophic nitrate uptake. These results suggest that exopolymer production and cycling may be more important to open ocean carbon biogeochemistry and the biological pump than previously expected.

1 Introduction

Subtropical oceans constitute one of earth's largest biomes, where the euphotic water column exhibits sustained macronutrient limitation due to strong thermal stratification (Reygondeau et al., 2013). Consistently low euphotic zone chlorophyll concentrations observed in these regions lead to depressed primary production estimates using ocean-colour satellite and bio-optical float profile data (Longhurst et al., 1995; Long et al., 2021; Westberry et al., 2023). Despite this assumption of low productivity, various measured rates of annual net community production (NCP) and total annual carbon export from the ocean subtropics suggest a biological pump strength that is maintained at levels consistent with mesotrophic oceanic regions receiving a higher vertical nutrient injection flux (Gruber et al., 1998; Emerson, 2014; Teng et al., 2014; Roshan and DeVries, 2017; Quay et al., 2020; Karl et al., 2021; Quay and Stephens, 2025).

Moderate rates of summertime surface dissolved inorganic carbon (DIC) drawdown are observed in low-chlorophyll Atlantic and Pacific subtropical oceans (2-3 mol C m^{-2} y^{-1}) despite limiting nitrate and phosphate concentrations, and stratification that would seem to limit diapycnal supply of nutrients to the euphotic zone for most of the year (Sambrotto et al., 1993; Michaels et al., 1994; Dave and Lozier, 2010; Williams et al., 2013; Emerson, 2014). Processes of nutrient enrichment such as N_2 fixation, episodic mixing events, and iron-rich dust deposition are unable to fully provide sufficient nutrient supply to sustain this persistent summertime anomaly (Johnson et al., 2010; Chow et al., 2017; Fawcett et al., 2018; Letscher and Villareal, 2018; Letelier et al., 2019; Karl et al., 2021). In addition, most subtropical regions exhibit subsurface respiration without concomitant nitrate release expected from the remineralization of Redfieldian organic matter. This produces a widespread negative preformed nitrate ($preNO_3^-$) anomaly between ~120-180m (Emerson and Hayward, 1995; Abell et al., 2005; Ascani et al., 2013; Letscher and Villareal, 2018; Smyth and Letscher, 2023), and stoichiometrically balanced positive $preNO_3^-$ anomalies found within the upper 100m where O_2 is produced without stoichiometric NO_3^- drawdown (Letscher and Villareal, 2018). The introduction of allochthonous macronutrient supply to the surface mixed layer by vertically migrating phytoplankton or the production and export of non-Redfieldian organic matter (high elemental carbon:nitrogen ratio) are two potential processes which may couple these three phenomena and help explain the elevated surface DIC drawdown and positive $preNO_3^-$ as well as negative $preNO_3^-$ below the sub-surface chlorophyll maximum in these regions (Letscher and Villareal, 2018) .

Transparent exopolymer particles (TEP), mostly comprised of acidic polysaccharides, are ubiquitous throughout the oceans, where they tend to accumulate in surface waters due to their low density (Azetsu-Scott and Passow, 2004). Exopolymers are typically observed as being carbon-rich, with C:N ratios of >20:1 (Mari et al., 2001; Engel and Passow, 2001; Passow, 2002b; Guo et al., 2022), which makes them a candidate for surface mixed layer DIC drawdown with minimal nitrogen requirement, particularly if composed of pure carbohydrate (e.g. 1 C : 1 O_2 : 0 N). While most abundant during large blooms of phytoplankton in eutrophic waters, TEP and their precursors are produced by a wide variety of phytoplankton and bacteria across different marine and aquatic environments (Passow et al., 1994; Nosaka et al., 2017; Zamanillo et al., 2019). Exopolymers act as a bridge between the dissolved and particulate fractions of marine organic matter, with dynamic assembly and disassembly of marine gels helping to fill the size continuum of particles in the ocean (Verdugo et al., 2004; Verdugo, 2012). The related but distinct Coomassie stainable particles (CSP) are thought to track the more protein-rich component of the marine exopolymer/gel pool, which likely impacts the fate of these particles differently

than the polysaccharide-rich TEP pool (Cisternas-Novoa et al., 2015; Zamanillo et al., 2021). TEP contributes to sinking exopolymer aggregates, which in turn constitute a significant flux of POC to the upper mesopelagic zone where much of this organic matter may be consumed by aggregate-associated bacteria (Wurl et al., 2011b; Nagata et al., 2021) and zooplankton (Ling and Alldredge, 2003).

TEP production from phytoplankton exudates is associated with excess DIC drawdown even in nutrient-replete water. In these regions, carbon overconsumption can be as high as 30-40% with respect to nitrate and phosphate removal and POM C:N:P stoichiometry (Toggweiler, 1993). Surface mixed layer exopolymer production may increase as cells are stressed by nutrient limitation or photo-oxidative stresses (Berman-Frank et al., 2007; Ortega-Retuerta et al., 2009a; Iuculano et al., 2017), persistent in many subtropical surface waters. Therefore, despite lower phytoplankton biomass in these oligotrophic regions, significant TEP production and seasonal variability may still occur.

Given that different oligotrophic regions exhibit significant variability in the elemental stoichiometry of organic matter including biomass (Martiny et al., 2013), detrital POM, and DOM (Letscher and Moore, 2015; Liang et al., 2023), across depth and time, region-specific measurements are needed to quantify the importance of exopolymer particles to pelagic biogeochemistry of different regions (McCarthy et al., 1996; Mari et al., 2001; Passow, 2002b; Beauvais et al., 2003).

In this study, we assess whether significant depth, temporal, and latitudinal gradients exist in: 1). exopolymer abundance and its associated C:N content that may help to explain the seasonal excess DIC drawdown in the absence of known nutrient supply pathways (e.g. Johnson et al., 2010), and 2) potentially related subsurface preNO_3^- anomalies present within the North Pacific subtropical gyre (NPSG). To do this, we sampled two classes of exopolymers: carbohydrate-rich transparent exopolymer particles (TEP) and protein-containing Coomassie-stainable particles (CSP) as well as dissolved carbohydrates (precursor molecules of larger exopolymer particles (Passow, 2000; Ortega-Retuerta et al., 2009b; Arnosti et al., 2021)), for nearly three years to quantify their concentrations, vertical distributions, and seasonal and latitudinal variability.

In order to produce quantitative estimates of TEP and CSP concentrations, we also directly estimated the organic C and N content of exopolymers spontaneously assembled under controlled conditions in the field to convert TEP and CSP values to carbon and nitrogen equivalents. With these quantitative estimates of TEP-C and CSP-N concentrations, we then discuss the potential contributions of the exopolymer cycle for explaining surface mixed layer excess DIC drawdown and subsurface preNO_3^- anomalies. This contribution helps to close the C, N, and O_2 budgets at station ALOHA, and may apply to the carbon and nutrient biogeochemistry of the subtropical oceans more generally.

Deleted: ,

2 Methods

2.1 Sample collection

Water samples for measurements of TEP, CSP, and dissolved polysaccharides were collected using a Niskin rosette onboard the RV *Kilo Moana* from 15 cruises between January 2020 and September 2022. 14 cruises were part of the Hawaiian Ocean Time-series (HOT) sampling program at Station ALOHA (22°

45’ N 158° W), with 1 cruise sampling 10 stations in the North Pacific Gyre along a nominal 158ºW transect from Station ALOHA to 31° N during June 2021, also on RV *Kilo Moana* (Fig. 1). Vertical profiles of salinity (Sea-Bird SBE-09), temperature (Sea-Bird SBE-3 Plus) and oxygen (Sea-Bird SBE-43) were also collected from the rosette CTD instrument package. Primary productivity, chlorophyll a, particulate carbon, and particulate nitrogen data measured as part of the HOT program for the period 1988-2022 were obtained from https://hahana.soest.hawaii.edu/hot/hot-dogs/.

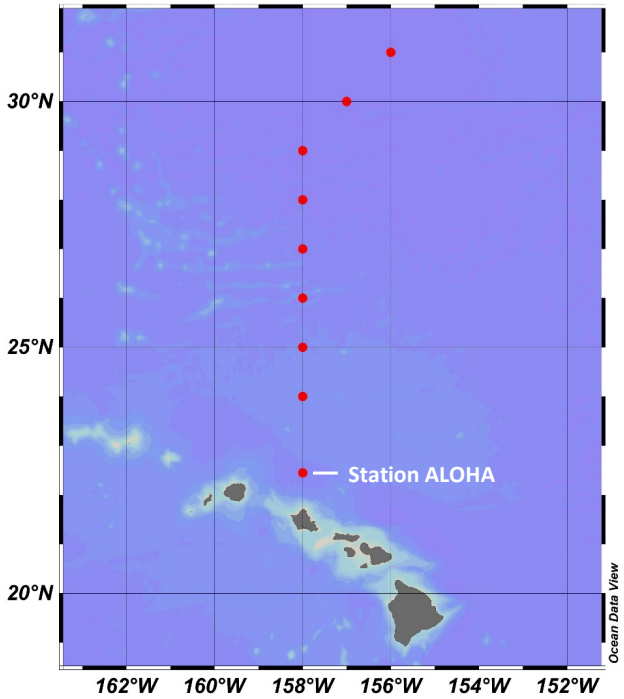

Figure 1. Map showing the location of Station ALOHA where time series measurements were collected and the stations along the June 2021 transect between ALOHA and 31°N.

2.2 Quantification of transparent exopolymer particles (TEP) and Coomassie-stainable particles (CSP)

Water samples for TEP and CSP (0.5-2.0L) were taken from 5-8 depths and stored in polycarbonate bottles (Corning) in blacked-out carriers until filtration. Samples were processed from deepest to shallowest to minimize any effects of small temperature changes on exopolymer formation dynamics. Water samples for TEP and CSP were filtered using 0.4 µm pore-size, 25mm diameter polycarbonate filters (Whatman) using a peristaltic pump (Cole-Parmer) and silicone tubing (Masterflex). Filters were then placed onto a vacuum filtration rig and dyed with acidified (pH 2.5) 0.02% Alcian Blue (AB) solution (Alcian Blue 8X, Sigma Aldrich) for TEP samples following Bittar et al. (2015) and 0.04% Coomassie brilliant blue (CBB)

(SERVA) solution (pH 7.4) for CSP samples following Cisternas-Novoa et al. (2015). Dyed filters were placed in polypropylene vials (Falcon) and frozen at -20ºC, and 2-day shipped back to the shore-based laboratory in ice-packed coolers (Pelican). TEP samples were extracted in 6 ml 80% sulphuric acid solution for 2 hrs and absorbance read at 787nm. CSP samples were extracted in 4 ml 3% sodium dodecyl sulphate (SDS) in 50% isopropyl alcohol solution for 2 hrs at 37°C under ultrasonication and read at 615nm. Absorbance values were blanked against the same type of polycarbonate filters after filtration of 500ml ultrapure water. Blanks were also taken with 500ml 0.2 µm filtered seawater to check that there was no bias resulting from sub-0.2 µm organic material from seawater retained on the filters. These blanks were not significantly different and had a combined coefficient of variation of 0.039. Absorbance values were calibrated against a dilution series of xanthan gum (XG) (Sigma) and bovine serum albumin (BSA) (Sigma) for TEP and CSP respectively. Concentration units are therefore expressed as µg XG equivalents L^{-1} and µg BA equivalents L^{-1} following the literature convention (e.g., Cisternas-Novoa et al. (2015)) using the spectrophotometric method for TEP and CSP quantification in Figure 2. TEP sample replicates had a mean coefficient of variation of 0.04 µg XG equiv. L^{-1} and CSP samples 0.14 µg BA equiv. L^{-1} (n=24) from 8 sets of triplicate measurements.

2.3 Dissolved carbohydrates

Water samples for dissolved carbohydrate analysis were gravity filtered from the Niskin rosette using a 47mm combusted GF/F filter (Whatman; 0.7µm nominal pore size) into acid cleaned and furnaced glass vials. Vials were frozen at -20ºC and transported similar to above for lab analysis. Using the approach of Myklestad et al (1997), total HCl-hydrolysable carbohydrates (TCHO) were measured against a glucose calibration standard and expressed in µM carbon. The method uses the alkaline ferricyanide reaction with 2,4,6-tripyridyl-*s*-triazine (TPTZ) that produces a deep violet color with reduced iron, allowing sensitive measurement of low carbohydrate concentrations with spectrophotometry. Reagents were made fresh for each run of samples and kept in blacked-out glassware. Coefficients of variation averaged 2.5% on triplicate analyses of dissolved carbohydrate.

2.4 Carbon and Nitrogen conversion factors

During field sampling at station ALOHA (22.75°N, 158°W) and from 31° N, 156°W in June 2021 and October 2021 from station ALOHA alone, 3 x 10 litre volumes of seawater from two depths (5m, 125m) were filtered through a 0.2 µm capsule filter (Pall) into opaque HDPE plastic bottles and stored in the dark while at sea at sample depth temperature ±1°C. Bottles were left for 80-100 hrs to allow sufficient time for exopolymer to spontaneously reform from the dissolved fraction. From these bottles, duplicate filtrations (1.5L) were performed for TEP and CSP concentrations as above and duplicate filtrations for particulate carbon and nitrogen were taken onto 47mm GF filters (Whatman) for CHN analysis of the collected exopolymer particles.

Particulate carbon and nitrogen data (in µM C and µM N) were then used with the measurements of TEP and CSP (in µg XG equiv. L^{-1} and µg BA equiv. L^{-1}) to convert the latter exopolymer concentration units to µM C and µM N using carbon and nitrogen conversion factors (CCF and NCF).

$$CCF = \frac{\mu M\ Particulate\ Carbon}{\mu g\ XG\ equiv\ L^{-1}} \quad (1)$$

$$NCF = \frac{\mu M\ Particulate\ Nitrogen}{\mu g\ BA\ equiv\ L^{-1}} \quad (2)$$

TEP carbon (TEP-C) and CSP nitrogen (CSP-N) concentrations are thereafter converted and expressed in µM units of carbon and nitrogen respectively.

3 Results

3.1 Carbon and Nitrogen conversion factors

Table 1. TEP-C and CSP-N conversion factors and exopolymer C:N ratios measured from exopolymer ingrowth incubations of 0.2 µm-filtered seawater conducted in June and October '21 at station ALOHA and at the northern end of the June '21 transect (31°N, 156°W); values in parentheses are coefficients of variation.

Conversions	TEP-C Jun 21	TEP-C Oct 21	CSP-N Jun 21	CSP-N Oct 21	C:N Jun 21	C:N Oct 21
ALOHA 5 m	0.529 (0.02)	0.577 (0.02)	0.018 (0.03)	0.012 (0.18)	25.7 (0.01)	18.54 (0.16)
ALOHA 125 m	0.627 (0.05)	0.600 (0.19)	0.005 (0.23)	0.013 (0.27)	34.3 (0.11)	16.40 (0.36)
31°N 5m	0.656 (0.12)		0.004 (0.05)		33.2 (0.04)	
31°N 125m	0.759 (0.05)		0.003 (0.19)		38.1 (0.01)	

Field Code Changed

Carbon conversion factors for TEP-C at station ALOHA varied between 0.529-0.627 µM C per µg XG equiv L^{-1} with mean surface values being lower than at 125 m ($p = 0.07$, Welch's t-test) (Table 1). These values are consistent with the frequently used conversion factor of 0.6 from Engel and Passow (2001). Nitrogen conversion factors for CSP-N varied by a factor of ~6 between 0.003-0.018 with lower organic nitrogen content found at 31ºN than at station ALOHA ($p = 0.04$, Welch's t-test) (Table 1.). The C:N ratio (16.4-34.3) at ALOHA varied more than carbon conversion factors (0.529-0.627), e.g. by a factor of ~2 and ~1.2 respectively, with summertime samples from 125 m being most carbon-rich and samples from October at 125 m having the lowest C:N ratios ($p = 0.007$, Welch's t-test). All samples were carbon-rich with respect to the canonical Redfield ratio, with exopolymer C:N ratios at station ALOHA being significantly higher in summer than autumn at 5 m ($p = 0.025$, Welch's t-test) and 125 m ($p = 0.007$, Welch's t-test), consistent with the observations of (Michaels et al., 1994). Summertime C:N ratios were significantly higher in northern gyre-associated waters (31°N) than at station ALOHA, e.g. 33 – 38 vs. 26 – 34, both for 5 m ($p = 0.0001$, Welch's t-test) and at 125 m ($p = 0.01$, Welch's t-test).

3.2 Interannual variation in TEP, CSP, and TCHO at station ALOHA

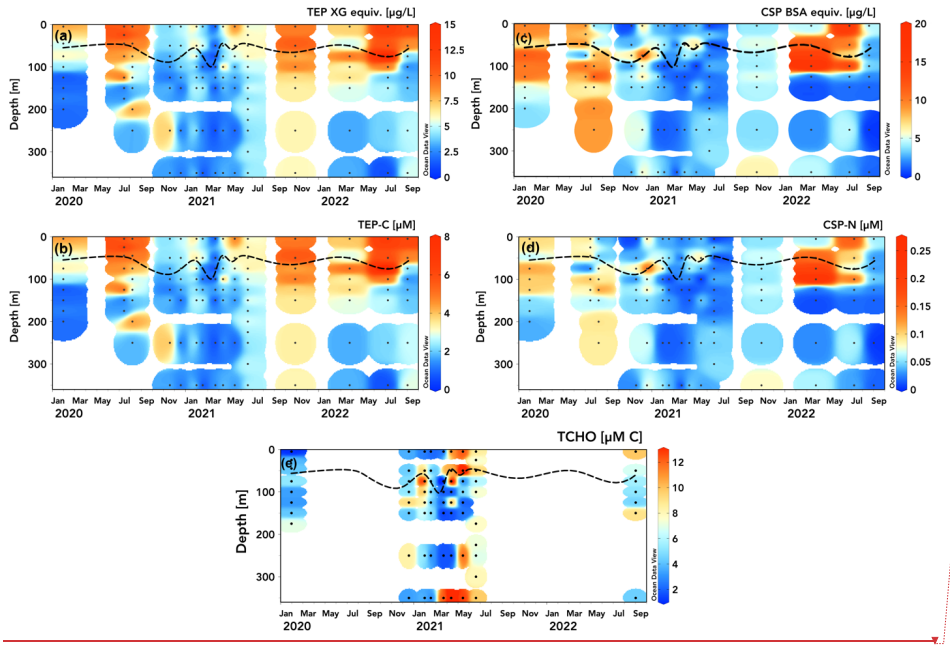

Deleted:

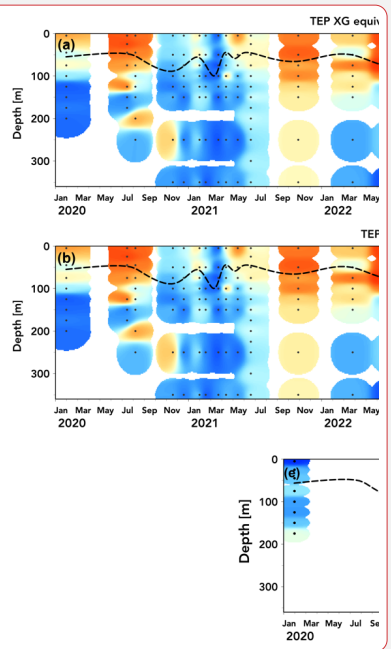

Figure 2. Station ALOHA time series (2020 – 2022) of TEP and CSP concentrations measured in xanthan gum (XG) (a) and bovine serum albumin (BSA) µg equivalents per litre (c) and converted to µM C (b) and µM N (d). Dissolved total carbohydrates (TCHO) concentrations [µM C] measured on select cruises presented in (e). Dashed line shows mixed layer depth calculated from HOT CTD data as 0.125°C decrease in temperature from the 10 m value.

At station ALOHA, TEP concentrations were highest during the summer months where values peaked within the surface mixed layer (8 – 15 XG equiv µg L^{-1} (Fig. 2a); 4 – 8 µM C (Fig. 2b)), with decreasing TEP concentrations below to underlying mesopelagic waters (1 – 5 XG equiv µg L^{-1} (Fig. 2a); 0.5 – 3 µM C (Fig. 2b). TEP concentrations were generally lower (2 – 7 XG equiv µg L^{-1}; 1 – 4 µM C), with less pronounced vertical gradients during winter months, suggesting either export of accumulated TEP from surface waters or a background of non-seasonal production or abiotic formation in deeper waters. Interannual variation in TEP concentrations in the upper 300 m is approximately 15 – 40% (coefficient of variation), with May – July 2021 having lower concentrations than similar periods in 2020 and 2022. March 2021 exhibited the lowest upper 100 m concentrations (coinciding with deepening of the surface mixed layer to 110 m after a series of storms and heavy rainfall).

The CSP distribution at station ALOHA exhibited a less observable seasonal pattern and less distinct vertical gradients as compared to TEP (Figure 2c, 2d). Elevated CSP concentrations appear to be distributed differently than TEP with high concentrations (6 – 18 BA equiv µg L^{-1} (Fig. 2c); 0.1 – 0.2 µM N (Fig. 2d)) found below the surface mixed layer (50 – 100 m) and around the top of the subsurface chlorophyll max (100-125 m), consistent with the general distributions measured by Cisternas-Novoa et al. (2015) for the Sargasso Sea. CSP in 2021 was 2 – 8 BA equiv µg L^{-1}; 0.01 – 0.07 µM N throughout the

upper 300 m, similar to subsurface chlorophyll max and mesopelagic (>125 m) CSP concentrations in 2020 and 2022, lacking an upper ocean seasonal peak (Fig. 2c, 2d). As with TEP, CSP concentrations were observed to be greater in March 2022 than post-storms in March 2021.

Total carbohydrate (TCHO) samples were taken on fewer HOT cruises than TEP and CSP samples during 2020-2022 due to logistical constraints. Total dissolved carbohydrates serve as a precursor substrate for the abiotic assembly of exopolymer particles in situ (Verdugo et al., 2004). TCHO concentrations varied between ~2 – 12 µM C across depths and season (Fig. 2e). There is a marked difference in the distribution of TCHO concentrations between winter samples in 2020 and 2021 where surface concentrations were low (2 – 6 µM) and data from spring 2021, where concentrations are consistently high at 350 m and in the upper 50 m from April through June (> 10 µM). Compared to DOC measurements taken at station ALOHA, this spring maximum at 350 m seems erroneous, but falls within the intra-annual variability of DOC at 350 m at ALOHA (± 6 µM C) and monthly variation in particulate export (Karl et al., 2021). It may be possible that some hydrolysable particulate polysaccharides are drawn through combusted GF/F filters (Nagata et al., 2021). Another potential explanation is the degradation and/or solubilization of exopolymers below the subsurface chlorophyll max where polysaccharide-specific enzyme activity is elevated (Reintjes et al., 2020).

3.3 Climatologies of TEP-C and CSP-N with Particulate Carbon and Nitrogen

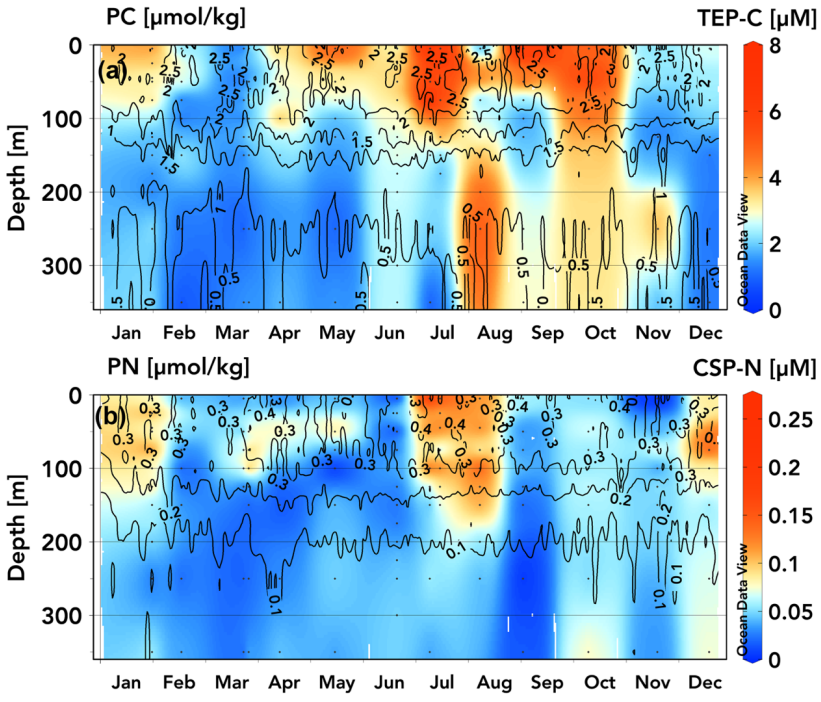

Figure 3. TEP-C (a) and CSP-N (b) (μM) concentration climatologies for 2020-2022 data measured at station ALOHA overlayed with contours from climatologies of particulate carbon (a) and particulate nitrogen (b) (μmol/kg) from the Hawaiian Ocean Time-series dataset (1989-2020 data).

Previous analyses of the climatology of upper ocean positive $preNO_3^-$ and subsurface negative $preNO_3^-$ anomaly generation at station ALOHA have revealed repeatable seasonal ingrowths of the respective anomalies during the months of April through November (Letscher and Villareal, 2018). These seasonal ingrowths are a common feature of these anomaly generation patterns across the northern hemisphere subtropics observed in the BGC-Argo float record (Smyth and Letscher, 2023). To explore exopolymer accumulation and vertical export as an explanation for these seasonal $preNO_3^-$ anomaly generation patterns, we converted the 2020-2022 TEP and CSP data to a monthly averaged climatology for station ALOHA (Figure 3), with the caveat that some months were only sampled once over the observational period. TEP exhibits a seasonal pattern with elevated concentrations found in the upper 100 m beginning in April/May (3 – 4 μM) increasing to an annual maximum in late June through early October (5 – 8 μM), followed by a decrease towards an annual minimum in February/March (1 – 2 μM) (Fig. 3a). TEP concentrations below 100 m are ~1 – 2 μM from December through June, increasing to 2 – 4 μM from June through November, concurrent with the seasonal maxima in upper 100 m TEP. We speculate that these moderate concentrations of TEP below 100 m present during summer/autumn may be due to slowly sinking aggregates as TEP accumulates in the upper 100 m through spring-summer and form aggregates before sinking, consistent with the contemporaneous peak in particulate export rates of ~30-55 mg C m^{-2} d^{-1} at station ALOHA (Emerson et al., 1997; Karl et al., 2012; Böttjer et al., 2017; Karl et al., 2021). The CSP climatology suggests two seasonal concentration maxima in the upper 100 – 130 m occurring in July/August and in December/January (0.07 – 0.13 μM) (Fig. 3b). CSP concentrations in other months and below these depths are <0.06 μM.

3.4 Patterns of TEP and CSP with respect to particulate C and N at station ALOHA

Comparing TEP and CSP concentrations to climatologies of particulate carbon (PC) and nitrogen (PN) respectively at station ALOHA (1989-2020; isolines in Fig. 3a, 3b) it is apparent that measured TEP concentrations reflect variation in euphotic PC more closely than CSP does PN, particularly for samples taken May-October. Elevated CSP-N concentrations during summer months (0.12-0.24 μM N) correspond with PN maxima, but during winter and spring, CSP-N comprises a smaller proportion of PN.

While CSP-N concentrations are lower in magnitude to PN concentrations, TEP-C is frequently observed to exceed background PC concentrations at station ALOHA, which may be an artifact of filtrations for PC and PN analysis losing exopolymers during GF/F filtration or excess dye binding to particles when using the colorimetric method of measuring TEP and CSP (Passow, 2002b; Bar-Zeev et al., 2011; Annane et al., 2015; Ortega-Retuerta et al., 2019; Nagata et al., 2021). The difference in nominal pore size between GF/F filters used to sample PC (0.7 μm) and the 0.4 μm pore-size polycarbonate filters used for TEP may also lead to sampling errors when comparing TEP-C and PC/POC, as most of these particles are small (<3 μm diameter) particularly in the upper 200 m, with particles tending larger as they age or sink and aggregate through the mesopelagic (Engel et al., 2020). It is therefore likely that TEP-C to PC ratios vary with depth and are more accurate for samples containing larger particles. Strands of microgels and larger particles may be easily pulled through GF/F filters under vacuum pressure and may be disaggregated when sampled in standard sediment catching methodology due to turbulence, break up at saline density layer, solubilization or rapid remineralization or preferential consumption by motile organisms (Smith et al., 1992; Buesseler et al., 2007; Fawcett et al., 2018). In addition to the variable size spectrum of TEP particles,

the electrochemistry that allows the aggregation of polymers into micro and macroscopic gels (principally divalent cations Ca^{2+} and Mg^{2+}) may be affected during filtration, and to a different degree with various polycarbonate and GF/F filters (Chin et al., 1998; Meers et al., 2006). If this is the case, then gels >0.4 µm that would otherwise be retained may be broken apart into constituent polymers or smaller nanogels that can pass through the filter. This would lead to TEP being quantified in the DOM fraction and lead to an overestimate of dissolved to particulate fractions of organic matter.

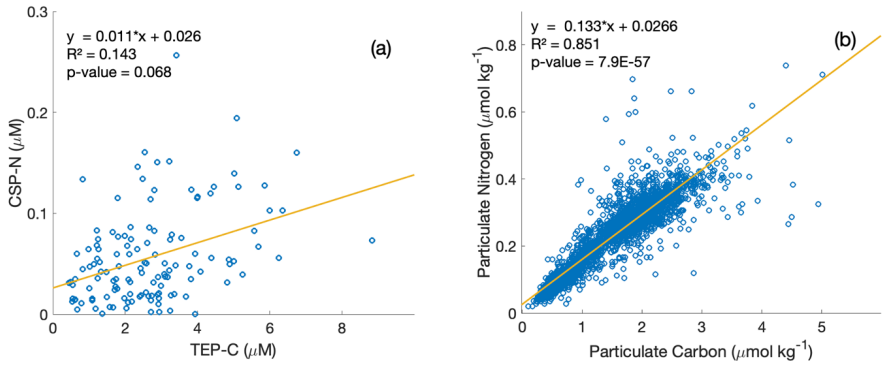

Figure 4. Property-property plots of measured CSP-N and TEP-C concentrations [µM] within the upper 350 m at station ALOHA from this study (a) and particulate nitrogen to particulate carbon [µmol kg^{-1}] from the HOT dataset (1989-2020 data) (b), including model II linear regression lines and correlation statistics.

We further explore the relationships between the exopolymer particle fraction, PC, and PN, and their respective stoichiometries with property-property plots (Fig. 4). PN and PC concentrations are well correlated (R^2 = 0.851, Model II regression) at station ALOHA (Fig. 4b) and the mean C:N ratio computed from the inverse of the slope (7.55) is slightly higher than the canonical Redfield ratio (6.63). In contrast, TEP-C and CSP-N concentrations show a weaker correlation (R^2 = 0.143, Model II regression), with an empirical estimate of the exopolymer particle C:N stoichiometry of 90.9 or 37.3 when the regression slope is forced through zero, the latter similar to the C:N stoichiometry determined directly on collected exopolymers (Table 1). The weaker correlation of TEP-C with CSP-N concentrations, due to the larger variability of the data, suggests different formation, consumption, and/or export dynamics for each group of exopolymers, consistent with the observations of Cisternas-Novoa et al. (2015) and Zamanillo et al. (2021).

3.5 TEP and rates of primary production

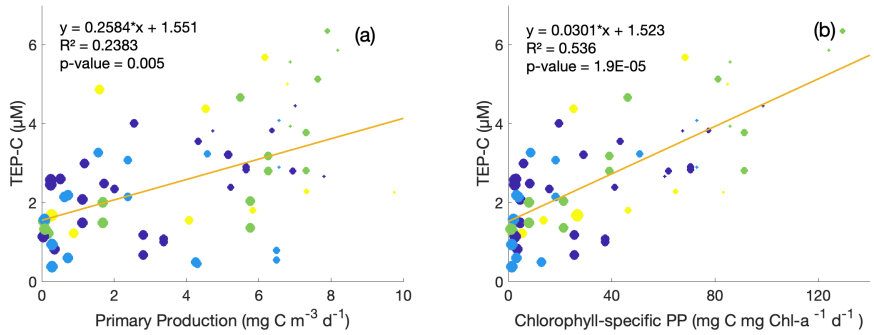

Figure 5. Property-property plots of measured TEP-C concentrations [µM C] within the upper 350 m from this study against same-depth daily primary production (a) and chlorophyll-specific primary production (b) measured at station ALOHA. Circle size indicates depth: larger circles are deeper samples. Colour denotes season: Purple = winter, Blue = Spring, Green = Summer, Yellow = Autumn. Model II linear regression lines and correlation statistics are provided.

As TEP production, abiotic formation, and consumption / degradation dynamics are often attributed to phytoplankton community structure and downwelling irradiance intensity (Zamanillo et al., 2019; Bar-Zeev et al., 2011; Ortega-Retuerta et al., 2009a; Berman-Frank et al., 2007; Passow, 2002a), daily primary production (PP) measurements taken during HOT cruises were compared with TEP concentrations, indicating a weak positive correlation for overall PP (R^2 = 0.24, Fig. 5a) and a stronger correlation for chlorophyll-normalized PP (R^2 = 0.54, Fig. 5b). The co-occurrence of higher TEP-C concentrations and high chlorophyll-specific primary production values in surface waters despite nutrient limitation may be indicative of enhanced release of TEP carbohydrate precursors in addition to downregulation of photosynthetic pigment synthesis in light-saturated surface waters (Rabouille et al., 2017; Thompson et al., 2018). The highest values of primary productivity and TEP concentration (>4 µM) were observed in Summer and Fall samples. There are too few data to determine whether TEP-C to PP ratios vary with season (coloured circles, Fig. 5). CSP-N showed no such correlations with primary production within this dataset. Although these results may be expected simply from the vertical gradients observed in TEP at station ALOHA, chlorophyll-normalized PP gives some information on whether TEP concentrations are only associated with surface accumulation or around the peak in chlorophyll at the subsurface chlorophyll max. While this small dataset of TEP and PP matchups may indicate TEP production is occurring around the subsurface chlorophyll max owing to moderate chlorophyll-normalized PP and TEP concentrations at these depths, there are too few data at present to draw firm conclusions, particularly for near-surface water. Wurl et al. (2011) found a similar disconnect between microbial activity and exopolymer distributions: variations in measured TEP production rates across different Pacific waters (including late-summer samples from station ALOHA) were not associated with phytoplankton blooms, changes in chlorophyll concentrations or fluorescence, with abiotic formation of TEP easily maintaining observed concentrations in the surface mixed layer (8-12 µM C L^{-1} d^{-1}).

3.6 TEP, CSP, and TCHO concentrations on June transect 22.75°N to 31°N

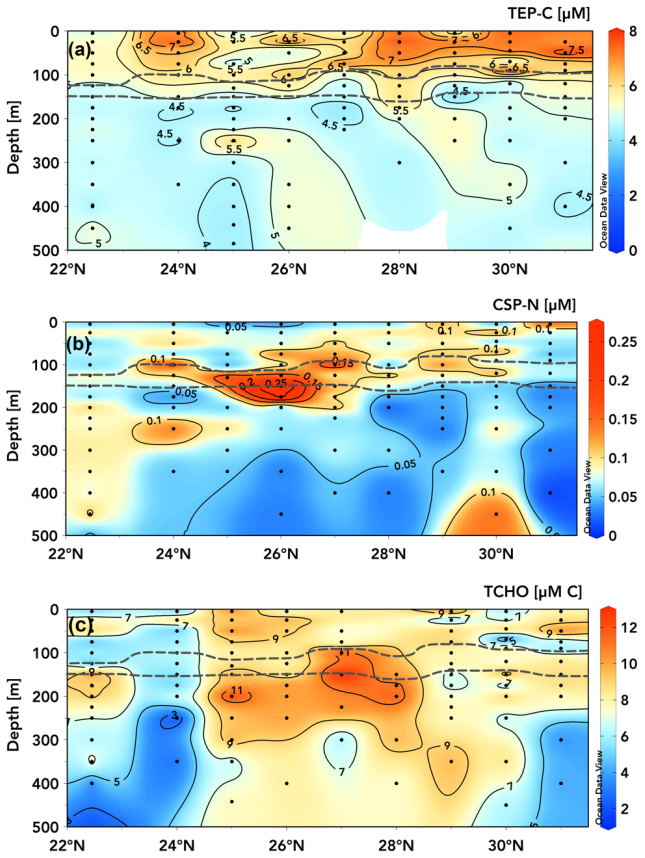

Figure 6. TEP-C [µM C] (a), CSP-N [µM N] (b), and TCHO [µM C] concentrations (with contour lines shown) within the upper 500 m measured during the June 2021 transect from 22.75°N to 31°N along ~158ºW. Dashed gray lines bound elevated CTD-mounted fluorescence, indicating the deep chlorophyll maximum.

The meridional transects of TEP-C and CSP-N concentrations in the upper 500 m taken between 22.75°N and 31°N along ~158ºW (Fig. 6) during June 2021 show an increase in upper ocean (above the subsurface chlorophyll max (gray lines, Fig. 6) TEP concentrations towards the gyre centre (Fig. 6a), with two occupations of station ALOHA at the beginning and end of the transect, separated by ten days having the lowest integrated TEP concentrations and degree of vertical gradient. From 24-31°N all stations exhibited pronounced vertical gradients in TEP concentrations between the surface and below the subsurface chlorophyll max on the order of ~2-3 µM TEP-C. At stations 24ºN and 28°N, moderate TEP-C concentrations (5.5 – 7 µM) extended into the subsurface chlorophyll max whereas high concentrations (6 – 8 µM) were restricted to the upper 75 m at 29°N and 31°N. It is unclear whether these patterns are

attributable to variable TEP production and consumption rates across depths, the production of buoyant TEP that is retained in the surface ocean, surface turbulence and wind forcing either converging TEP to certain latitudes or variably acting to break apart TEP particles, or gradients in phytoplankton nutrient or oxidative stress, or photoacclimation responses affecting exudate production between sites (Sun et al., 2018; Prairie et al., 2019). It is also of note that most stations exhibited a local increase in TEP-C at ~10-20 m immediately above the top of the subsurface chlorophyll max. The surface maxima in TEP-C present at 28-31ºN was ~8 µM (Fig. 6a), similar in magnitude to the surface maxima accumulating seasonally in the station ALOHA time-series (Fig. 2a, 2b; 3a). However, the vertical TEP-C gradients encountered from 24-31ºN in June 2021 were ~2-3 µM, approximately half that observed seasonally at station ALOHA (Fig. 2b). The observed ~2 µM latitudinal gradient in 0-100 m TEP-C concentrations (e.g. ~5 µM to ~7 µM at 22.75º to 24ºN and similarly at 25º to 28 – 31ºN; Fig. 6a) may also be attributed to the build-up of less labile or less export-prone (or coagulation efficient) TEP as waters move towards the gyre interior (Mari et al., 2007; Rochelle-Newall et al., 2010; Mari et al., 2017), a feature that is also observed for the marine DOC pool (Hansell et al., 2009).

The meridional and vertical gradients in CSP-N concentrations (Fig. 6b) throughout the transect did not correspond to those of TEP-C (Fig. 6a). CSP-N concentrations were highest (0.15-0.26 µM) between 75-200 m for stations 24-29°N. Profiles at 22.75°N, 30ºN and 31°N were more uniform with moderate CSP-N concentrations (0.05 – 0.12 µM) observed below 250 m. Elevated CSP concentrations appear to be more closely associated with peak fluorescence signals within the subsurface chlorophyll max (gray lines) while TEP is most abundant in the surface waters above. This disconnect between TEP and CSP distributions suggests different dynamics in formation, residence time and decomposition and export process between the two classes of exopolymers (Grossart et al., 2006; Engel et al., 2015; Thornton, 2018).

Measured concentrations of total dissolved carbohydrates (TCHO) varied between ~2.5-13 µM C across the June 2021 transect (Fig. 6c). Elevated TCHO concentrations did show some overlap with elevated surface TEP concentrations but were not consistent with TEP concentrations below the subsurface chlorophyll max (Fig. 6c). At many stations, e.g. 25º – 28ºN, TCHO concentrations were elevated (9-12.5 µM) around and below the subsurface chlorophyll max, where TEP-C concentrations were low (4.5-5.5 µM C) but CSP-N concentrations were elevated (>0.015 µM N). Most stations exhibited vertical gradients between surface or subsurface chlorophyll max maxima (≥10 µM) and reduced TCHO concentrations (2 – 8 µM) below 250 m, but some stations were more consistent with depth (24°N, 29°N) with peak values near the surface. These patterns are generally dissimilar to TEP distributions that are elevated in surface waters. Measurements from this study were on the lower end of marine dissolved carbohydrate measurements, but consistent with previous measurements taken within the subtropical North Pacific (Pakulski and Benner, 1994), 30-60% lower than observed across the subtropical Atlantic (Burney et al., 1979; Goldberg et al., 2010) and 40-100% higher than in the Bay of Bengal and Arabian Sea (Bhosle et al., 1998).

4 Discussion

4.1 TEP, CSP, TCHO, and exopolymer C:N stoichiometry patterns at station ALOHA

A major motivation for this study of exopolymer particle dynamics at station ALOHA was to assess the potential for this organic matter pool to help explain the shallow subsurface negative, and euphotic zone positive, preNO_3^- anomalies and DIC drawdown at this site, which have thus far evaded complete accounting in the relevant tracer budgets of carbon, oxygen, and nutrients (Johnson et al., 2010; Letscher and Villareal, 2018). DIC drawdown from the surface mixed layer at station ALOHA occurs from ~April through October (Keeling et al., 2004), a period of the seasonal cycle that coincides with positive preNO_3^- anomaly generation in the lower euphotic zone (~40-100 m) and negative preNO_3^- anomaly generation below (~100-180 m) that are in approximate stoichiometric balance (Letscher and Villareal, 2018). These preNO_3^- anomalies suggest biogeochemical processes acting on the oxygen and nitrate pools that produce O_2 with little nitrate drawdown in the lower euphotic zone and oxygen consumption with little accumulation of nitrate below in the shallow mesopelagic. Surface ocean production/accumulation of exopolymer particles and their export and subsequent remineralization below the shallow mesopelagic is one candidate biogeochemical process that could help explain the preNO_3^- anomaly generation as well as surface mixed layer DIC drawdown in the absence of nutrient injection. This would be supported if seasonal patterns of these exopolymer dynamics match the April through October timing of peak DIC and preNO_3^- changes and if the exopolymer particle pool exhibits elevated C:N stoichiometry which drive comparatively larger changes in the DIC and O_2 pools than nitrate.

We observe a seasonal pattern for TEP concentrations at station ALOHA that includes elevated concentrations (~4-8 µM C) above ~100 m in the late spring through early fall months, with lower concentrations (~1-3 µM C) at these depths in November through March, especially in 2020-2021 (Fig. 2a, 2b), which are similar to TEP concentrations at ~100-350 m throughout the year. CSP concentrations are generally similar in pattern, however there are notable differences such as slightly deeper upper ocean maxima (e.g. from the surface down to ~120 m) and earlier seasonal peaks in the late winter early spring and seasonal lows (ending by Sep) in the upper 100 m (Fig. 2c, 2d). The limited data on the exopolymer precursor pool of dissolved TCHO precludes a complete description of the seasonal cycle, however the most elevated concentrations (~8-12 µM C) in the upper ~100 m found in early 2021 immediately precede the growth of the seasonal peak in TEP that year beginning in May (Fig. 2e, 2b). Viewed as a monthly climatology (Fig. 3a), TEP concentrations in the upper 100 m are at the annual minimum in November through March (< 3 µM C), begin to increase in concentration from April to July, and are maintained at elevated concentrations of ~4-8 µM C through October. TEP concentrations below 100 m are low (<3 µM C) year-round with the exception of some intermediate concentrations (~3-5 µM C) in the ~100-350 m depth range in July through October (Fig. 3a), more present in 2020 and 2021 than in 2022 (Fig. 2b). The seasonal upper 100 m peak in CSP is restricted to July and August in the monthly climatology (Fig. 3b) with a wintertime peak also observed (Dec – Jan), more present in 2020 than 2021 or 2022 (Fig. 2d). The empirically estimated C:N stoichiometry of the exopolymer pool in the upper 125 m is ~1.4-2.1 times more C-rich/N-poor in June 2021 than October 2021 (Table 1), suggesting that the seasonal cycles of TEP and CSP may drive a seasonal cycle in exopolymer particle stoichiometry with the most N-poor material found during summer months. All of the above seasonal patterns in euphotic zone and upper mesopelagic TEP, CSP, and exopolymer particle stoichiometry are consistent with these pools potentially helping explain the April through October patterns of surface mixed layer

Formatted: Font color: Text 1

DIC drawdown, euphotic zone positive $preNO_3^-$, and subsurface negative $preNO_3^-$ anomalies at station ALOHA.

4.2 Contribution of TEP production to net community production and $PreNO_3^-$ anomalies

Here we use the seasonal study of TEP distributions from the upper 350 m at station ALOHA to quantify its potential contribution to help explain the dual enigmas of significant net community production (DIC drawdown) from the surface mixed layer in the absence of large vertical nutrient inputs and the generation of $preNO_3^-$ anomalies within and immediately below the euphotic zone of the subtropical North Pacific. The potential contribution of TEP to surface excess DIC drawdown and subsurface negative $preNO_3^-$ anomalies under nutrient limitation has been previously identified through field and lab observations (Mari et al., 2017; Fawcett et al., 2018; Letscher and Villareal, 2018; Nagata et al., 2021). The seasonal ~4-6 µM TEP-C concentration gradient observed between Apr-Oct in the upper 100 m and the waters below in this study at station ALOHA, may account for a significant contribution of TEP/exopolymer particles to both the seasonal mixed layer net community production and upper ocean $preNO_3^-$ anomalies through the processes of TEP production, sinking or matter exported during winter mixing, and subsequent remineralization at depth. TEP may have a significant role in exporting low-N organic matter to underlying waters, particularly during the summer to early autumn months (Fig. 3) when the seasonal maximum in upper 100 m TEP concentrations extends vertically into the 100 – 300 m layer, suggestive of vertical sinking.

The 4-6 µM vertical TEP gradient that arises seasonally at station ALOHA , e.g. 5-8 µM in the upper 100 m Apr-Oct decreasing to 1-2 µM below, is higher than that observed by Cisternas-Novoa et al (2015) (~10 µg XG equiv µg L^{-1} / ~0.5 µM TEP-C) in the Sargasso Sea and Wurl et al. (2011) (1.4-3.2 µM TEP-C with one high-TEP station with a gradient of 27 µM TEP-C) in the subtropical North Pacific when applying the carbon-converted units measured in this study. The wintertime erasure in vertical TEP gradients between the surface and 200 m is observed in Feb-Mar and Nov-Dec samples from station ALOHA in this study (Fig. 3a), supporting the hypothesis of TEP-C export to depth of ~100 m at ALOHA and possibly deeper at latitudes further north in the subtropical North Pacific, via the seasonal mixed layer pump which can deliver suspended particulate organic carbon (Dall'Olmo et al., 2016) and DOC (Hansell and Carlson, 2001) to sub-euphotic depths. This may operate in conjunction with the formation of sinking TEP aggregates which may occur year-round (Mari et al., 2017). As its C:N stoichiometry at station ALOHA was 40-110% greater for summer than autumn, it seems that exported exopolymer particles from the surface mixed layer to depths below may contribute disproportionally to positive and negative $preNO_3^-$ anomaly generation during the summer months at elevated C:N stoichiometry, meaning respiration associated with sinking exopolymers may have variable O_2 drawdown to nitrate release throughout the year.

The background particulate carbon flux at 150 m measured at station ALOHA of 27.8 ± 9.7 mg C m^2 d^{-1} (845 ± 295 mmol C m^{-2} yr^{-1}; Karl et al. 2021) would seem to indicate that the export of even a portion of the 0-150 m integrated 750 ± 150 mmol C m^{-2} summer/fall TEP stock by either TEP sinking or vertical export following winter mixing would be a significant flux of carbon on an annual scale. Furthermore, sediment trap data indicate that particulate matter exported at station ALOHA is typically slightly above Redfieldian C:N proportions, e.g. ~8.0 (Hannides et al., 2009), while TEP measured in this study varied between 16.4 in October to 34.3 in June (Table 1). The annual net community production rate estimated from the seasonal DIC cycle within the surface mixed layer (~50 m) at Station ALOHA is 2.3 ± 0.8 mol m^{-2} y^{-1} (Keeling et al., 2004), thus the annual production of a surface accumulated TEP-C stock of 0.2-0.3 mol

m^{-2} in the upper 50 m (e.g., ΔTEP = 4 – 6 mmol C m^{-3} multiplied by 50 m) may contribute 6.5-20% of the overall net community production estimated from DIC drawdown (e.g., 0.2-0.3 divided by 2.3 ± 0.8 mol C m^{-2} y^{-1}), if this material is exported below. The minimum contribution of TEP to mixed layer net community production is slightly lower, ~3.5% if the seasonal ΔTEP value of ~2 mmol C m^{-3} from 2020 is used.

From the calculation above, TEP production within and subsequent export below the surface mixed layer may explain up to 20% of the total net community production, but how does this estimate compare to the estimates of 'excess' DIC drawdown, that is DIC drawdown in excess of known N inputs (Johnson et al., 2010), at this site? For this calculation, it is helpful to compute the N demand required to produce the observed net community production rate, partitioned amongst the relative proportions explained by the production of POM and DOM. Johnson et al. (2010) computed a total N demand of 287 mmol N m^{-2} y^{-1} at station ALOHA assuming total organic matter production followed a C:N stoichiometry of 8.0, matching the sinking POM stoichiometry (Hannides et al., 2009). Letscher & Villareal (2018) empirically determined the fraction of net community production partitioned to DOM at station ALOHA from tracer budgets in upper mesopelagic isopycnal layers from the station ALOHA climatology, finding that ~50% of net community production is exported as DOM. We have computed the mean DOM C:N stoichiometry in the upper 200 m at 15.5 ± 1.3 from the same climatology. Assuming net community production is partitioned 50/50% between POM and DOM with C:N stoichiometries of 8.0 and 15.5 respectively, we compute a revised N demand of 218 mmol N m^{-2} y^{-1} to satisfy the observed 2.3 mol C m^{-2} y^{-1} net community production within the mixed layer (Keeling et al., 2004) for the scenario whereby only POM and DOM contribute to export production. Johnson et al. (2010) summarized total N supply to the mixed layer at station ALOHA finding a magnitude of 144 – 201 mmol N m^{-2} y^{-1}. Thus approximately 8 – 34% (mean = 21%) of the observed net community production N requirement is not accounted for by the known N supply (i.e. 'unexplained') for the scenario whereby only POM and DOM export contribute to net community production. Our study suggests that exopolymer particles may contribute as a third organic matter pool that can be exported to balance net community production. Our estimate of TEP production and its contribution to net community production at this site is 6.5 – 20%, with an observationally determined C:N stoichiometry of 16.4 – 34.3 (Table 1). Addition of TEP into the surface mixed layer net community production budget yields an N demand to explain TEP production of 4 – 28 mmol N m^{-2} y^{-1}, which reduces the revised total N demand of 218 mmol N m^{-2} y^{-1} (after accounting for elevated C:N DOM) even further downwards to 174 – 208 mmol N m^{-2} y^{-1}. Comparing this N demand to the prior calculated N demand that included POM and DOM but ignored TEP, TEP contributions to the upper ocean net community production budget help explain ~57% of the 'unexplained' excess DIC drawdown from the surface mixed layer, i.e. by reducing the overall unexplained drawdown from a mean of ~21% to ~9%, estimated from comparing the revised N demand for an upper ocean ecosystem including TEP production of 174-208 mmol N m^{-2} y^{-1} to the estimated N supply of 144-201 mmol N m^{-2} y^{-1} at station ALOHA (Johnson et al., 2010).

Deleted:

Table 2. Estimates of the nitrogen demand partitioned amongst POM, DOM, and TEP required to satisfy each fractional contribution (^{f}NCP) of the mixed layer 2.3 mol m^{-2} y^{-1} net community production at station ALOHA using their respective C:N stoichiometries. Total N supply is taken from Johnson et al. (2010) and includes vertical NO_3 fluxes plus N_2 fixation. $^{f}NCP_{POM}$ varies as the particulate fraction not attributable to TEP or DOM ($^{f}NCP_{POM}$ = 1-($^{f}NCP_{TEP}$ + $^{f}NCP_{DOM}$)), POM C:N from Hannides et al. (2009), $^{f}NCP_{DOM}$ from Letscher and Villareal (2018), DOM C:N from the upper 200 m average of the station ALOHA climatology, $^{f}NCP_{TEP}$ and TEP C:N (Table 1) from this study. N demand computed from 2.3 mol C m^{-2} yr^{-1} divided by C:N multiplied by ^{f}NCP.

Depth integration		[f]NCP	C:N	N demand (mmol N m^{-2} yr^{-1})	% of N demand
50m	POM	0.30-0.435	8	86-125	36-52
	DOM	0.5	15.5	74	31
	TEP	0.065-0.20	16.4-34.3	4-28	2-12
	Total demand			**174-208**	
	Total supply			**144-201**	

Lastly, we compare the seasonal TEP cycle observed at station ALOHA from 2020-2022 to previous estimates of the formation rates of residual preNO_3^- anomalies within and immediately below the euphotic zone. Letscher and Villareal (2018) estimated the seasonal (~Apr-Oct) development of a residual positive preNO_3^- anomaly (i.e. the residual anomaly after accounting for non-Redfield POM and DOM stoichiometry) within the upper 100 m with a climatological magnitude of 0.53 ± 0.27 µM N. A similar seasonal negative preNO_3^- anomaly develops between ~100-180 m with a climatological magnitude of -0.54 ± 0.25 µM N over a ~180-day period from Apr-Oct, consistent with surface TEP accumulation before winter mixing (Fig. 2). With an assumed 1:1 C:O_2 stoichiometry of TEP formation and remineralization (as for nearly pure carbohydrate material), the consumption of 4-6 µM seasonally exported TEP C (at a C:N ratio of 25 ± 8) should release the equivalent of 0.12-0.35 µM nitrate which is 23-67% of the 0.53 µM mean residual negative preNO_3^- anomaly and 22-64% of the 0.54 µM mean residual positive preNO_3^- anomaly. These values for TEP's potential contribution to preNO_3^- anomalies assume the export of surface TEP to underlying waters 100-200 m where they are subsequently remineralized. If a large proportion of seasonal TEP production is quickly exported to the deeper mesopelagic through aggregation and gravitational settling or winter mixing, then these values will likely be overestimates. Remaining mechanisms to explain the remainder of preNO_3^- anomaly formation include mining of sub-euphotic zone nitrate by vertically migrating phytoplankton (Pilskaln et al., 2005; Villareal et al., 2014) and heterotrophic bacterial uptake of nitrate when consuming C-rich organic matter such as TEP (Fawcett et al., 2018).

Finally, we note that moderate concentrations of TEP at 150-350 m (3-5 µM C) are present throughout the late summer to early autumn months at station ALOHA (Fig. 2b, Fig. 3a), but whether these concentrations represent matter exported from the surface or subsurface chlorophyll max below the depth of the negative preNO_3^- anomaly (~100 – 180 m; Letscher & Villareal, 2018), or separate activity in the upper mesopelagic is unclear. Compositional analysis of TEP molecules and polysaccharide-associated enzymes throughout the water column and over an annual cycle may elucidate sources and sinks of TEP beyond physical sinking and mixing processes.

4.3 TEP, CSP, and TCHO meridional patterns in the NPSG

Previous observations of TEP and CSP particle concentrations in high latitude oceans and temperate shelf seas have observed that both exopolymers are coupled to chlorophyll distributions (Beauvais et al., 2003; Busch et al., 2017; Nosaka et al., 2017; Anastasi, n.d.; von Jackowski et al., 2020). Other mid-latitude regions such as the Sargasso Sea (Cisternas-Novoa et al., 2015) and Catalan Sea (Zamanillo et al., 2021) exhibit different dynamics, where TEP is disconnected from CSP distributions as was observed in this study in the subtropical North Pacific.

Exopolymers measured across the upper 500 m of the subtropical North Pacific in June 2021 (Fig. 6) were found to have depth gradients similar to summertime conditions at station ALOHA (Fig. 2, 3), with elevated concentrations in surface waters for TEP and around the subsurface chlorophyll max for CSP and lower concentrations below in the shallow mesopelagic. There are also meridional gradients present (Fig. 6) with increasing surface ocean TEP concentrations northwards towards 31ºN while CSP is most elevated at 24 – 30ºN. Without additional data on TEP/exopolymer molecular composition it is difficult to ascertain whether this meridional gradient represents accumulation of more refractory TEP, or enhanced production/depressed export from waters towards 31ºN. However, this TEP meridional gradient matches that observed for surface ocean DOC in the region (Abell et al., 2000) which is thought to arise from the convergence of a semilabile component of DOC with lifetimes of years by the Ekman circulation across subtropical gyres (Hansell et al., 2009). The C:N stoichiometry of the exopolymer particle pool was also found to increase from station ALOHA to 31ºN both at the surface (~26 vs. ~33) and at 125 m (~34 vs. ~38) (Table 1). Dissolved TCHO were more elevated (> 7 µM C) north of 24ºN as well (Fig. 6c). The observed disconnect between TEP and TCHO distributions may be attributed to both formation and degradation processes: precursors being created around the subsurface chlorophyll max by phytoplankton and resultant low-density TEP particles concentrating in surface waters or sinking TEP being hydrolyzed below the subsurface chlorophyll max by bacteria, yielding reduced TCHO concentrations. The latter process is consistent with the hypothesized remineralization of low-N organic matter requiring heterotrophic nitrate uptake, generating a negative preNO_3^- anomaly (Fawcett et al., 2018). Compositional analysis of TEP particles, dissolved sugars, and stable isotopic measurements of the relevant nutrient and organic matter N contents through the upper 400 m would help confirm. Lastly, a lack of spatiotemporal coherence in the distributions of TEP and its precursor TCHO may result from differing timescales over which they are biotically cycled, with the latter possibly processed 3-10 times faster than other common labile organic materials like amino acids by bacteria in open ocean environments (Kaiser and Benner, 2012).

The meridional patterns observed in TEP, CSP, TCHO, and exopolymer particle C:N stoichiometry are all suggestive that the contributions of exopolymer particle dynamics to upper ocean net community production, export, and nutrient cycling diagnosed at station ALOHA (Sect 4.2) may play a larger role further north towards the core of the subtropical North Pacific gyre. While the TEP concentrations measured in this study were low (~2-15 XG equiv. µg/L; 1-8 µM C) compared to other regions (e.g. ~20-40 XG equiv. µg/L in the Sargasso Sea (Cisternas-Novoa et al., 2015); ~1-20 µM C in the tropical North Pacific (Wurl et al., 2011)), their highly carbon-enriched stoichiometry (particularly in summer with C:N = 26-38) means that these particles are a significant component of the upper ocean organic matter pool. The seasonal and latitudinal variation we observed in carbon and nitrogen conversion factors suggest using a single factor will bias many estimates of TEP-C and CSP-N from dye-binding assays. We therefore hope that more effort will be made in future studies to constrain TEP and CSP elemental stoichiometry to compare exopolymer concentrations from different depths, seasons and locations with greater confidence.

5 Conclusions and Future Directions

The seasonal, interannual and meridional variation of TEP and CSP observed in this study reinforces the building evidence that exopolymer production, accumulation and remineralization are not static processes, even in oligotrophic regions (Radić et al., 2006; Cisternas-Novoa et al., 2015; Engel et al., 2015;

Zäncker et al., 2017). Further process experiments that incorporate TEP and CSP dynamics with respect to other biological and chemical parameters are needed to understand the biogeochemistry of each exopolymer type for a given location and season, aiding efforts to model both with respect to other parameters through depth and time at a synoptic scale. Work that helps to validate the sources and sinks of exopolymers within the water column is particularly important in quantifying how much carbon is exported from or cycled within surface waters (including the surface microlayer) and where these molecules are remineralized. Compositional analysis of TEP particle and dissolved carbohydrates compositions and associated proteomic or transcriptomic analyses may elucidate the vertical distribution of TEP production, enzymatic hydrolyzation and remineralization of the resulting labile monomeric sugars.

TEP concentrations measured with the Alcian blue spectrophotometric method and converted to µM C with our empirically derived carbon conversion factors were found to be greater than GF/F collected particulate carbon measurements from the Hawaiian Ocean Time-series. Additionally, the estimated C:N stoichiometry of 16.4 – 38.1 for exopolymer particles from this study is significantly C-rich/N-poor relative to the C:N of the sinking flux collected in sediment traps at station ALOHA, 8.0 (Hannides et al., 2009). This supports the hypotheses that TEP and marine microgels may be 'missed' by traditional sampling techniques for sinking and suspended particulate organic carbon (Quigg et al., 2021), possibly due to disaggregation of the gel-particles upon encountering the GF/F filter or collection brine of sediment traps as well as potential rapid microbial remineralization within trap cups (Fawcett et al., 2018 and references therein). Future research is required to resolve the mechanisms leading to inefficient collection of TEP within standard marine particle sampling protocols and fully integrate TEP and marine gels sampling within marine carbon biogeochemistry studies. Further work is also needed to ascertain the degree to which exopolymer particles are exported below the surface ocean via slow gravitational sinking and/or vertical mixing within the seasonal mixed layer pump (Quigg et al., 2021; Mari et al., 2017).

Though TEP sinking rates, remineralization rates and C:O_2 respiration stoichiometry are not addressed in this dataset, previous studies in analogous regions indicate that the summertime production of highly non-Redfieldian exopolymers and potential winter export observed in this time series may explain a significant portion of subtropical positive and negative preNO_3^- anomalies (22-67%), consistent with this mechanism's description and modelling by Letscher and Villareal (2018). Uncertainty in the contribution of TEP/exopolymers to preNO_3^- anomalies (and excess DIC drawdown) primarily results from variability in the total TEP upper ocean accumulation and its C:N ratio; with some evidence for seasonal, vertical, and meridional differences in these ratios evidenced in this study. The upper ocean exopolymer cycle helps to close the C, N, and O_2 budgets at station ALOHA by contributing 8.5-20% of net community production and reducing the 'missing' mixed layer DIC drawdown and N supply by ~57% and ~12%, respectively. While leaving room for significant contributions from other processes such as vertically migrating phytoplankton and heterotrophic nitrate uptake to be further validated. More frequent measurements of TEP concentrations and its stoichiometry from the subtropical North Pacific and elsewhere would help quantify this potentially overlooked component of the ocean's biological pump operating across the vast subtropical gyres.

Deleted: Following the conversion of semi-quantitative measurements of exopolymers from dye-binding assays, our elemental conversions to C and N units allow us to estimate the magnitude of TEP's importance to surface ocean carbon dynamics on an annual cycle. We estimate that TEP accumulation within the ~50 m mixed layer may constitute 6.5-20% (0.2-0.3 mol m^{-2} y^{-1}) of the net community production (2.3 ± 0.8 mol m^{-2} y^{-1}) at station ALOHA. With its low N requirement, TEP reduces the overall N demand needed to explain the observed net community production at this site, bringing the measured N supply and demand into near balance. If TEP is sufficiently exported below the euphotic zone by a combination of sinking and/or winter vertical mixing, its cycling can reduce the unexplained 'excess' DIC drawdown from the mixed layer by ~57%, bringing the overall unexplained excess (or missing N supply) to ~9%. ¶

Deleted: ,

Deleted: w

Deleted: .

Author contributions

RTL and TV conceptualized this study as part of NSF grants 1923687 and 1923667 "Transparent exopolymer and phytoplankton vertical migration as sources for preformed nitrate anomalies in the

subtropical N. Pacific Ocean". KC, RTL, and HOT technicians performed fieldwork; KC performed laboratory analyses for TEP, CSP and TCHO and respective data analyses. KC, RTL, and TV contributed to writing and editing. Data from the Hawaiian Ocean Time series were obtained via the Hawaii Ocean Time-series HOT-DOGS application; University of Hawai'i at Mānoa. National Science Foundation Award # 1756517.

Acknowledgements

We would like to thank the crew and technicians aboard the RV Kilo Moana for their assistance in collecting samples through the COVID pandemic and assisting during the June 2021 transect cruise. We are grateful to Angelicque White (UH-Manoa) for her assistance and leadership in accommodating the TEP, CSP, and TCHO sampling on the 2020-2022 HOT cruises and to Brandon Brenes (UH-Manoa) for much of the sample collection at sea. We also wish to thank former UNH graduate students Jessica Gray and Sarah Benson for their assistance with sampling during the 2021 cruise.

Financial support

This study was funded as part of NSF grant 1923687 to RTL and 1923667 to TV entitled: "Collaborative research: Transparent exopolymer and phytoplankton vertical migration as sources for preformed nitrate anomalies in the subtropical N. Pacific Ocean."

Data availability

The data reported in this study are available at: https://www.bco-dmo.org/project/772658.

Competing interests

We declare no competing interests in the undertaking and publication of this study.

References

Abell, J., Emerson, S., and Keil, R. G.: Using preformed nitrate to infer decadal changes in DOM remineralization in the subtropical North Pacific, Glob. Biogeochem. Cycles, 19, https://doi.org/10.1029/2004GB002285, 2005.

Aller, J. Y., Radway, J. C., Kilthau, W. P., Bothe, D. W., Wilson, T. W., Vaillancourt, R. D., Quinn, P. K., Coffman, D. J., Murray, B. J., and Knopf, D. A.: Size-resolved characterization of the polysaccharidic and proteinaceous components of sea spray aerosol, Atmos. Environ., 154, 331–347, https://doi.org/10.1016/j.atmosenv.2017.01.053, 2017.

Anastasi, G.: OBSERVATIONS AND MODELLING OF TRANSPARENT EXOPOLYMER PARTICLES (TEP) AND THEIR ROLE IN CARBON CYCLING IN SHELF SEAS, 237, n.d.

Annane, S., St-Amand, L., Starr, M., Pelletier, E., and Ferreyra, G. A.: Contribution of transparent exopolymeric particles (TEP) to estuarine particulate organic carbon pool, Mar. Ecol. Prog. Ser., 529, 17–34, https://doi.org/10.3354/meps11294, 2015.

Arnosti, C., Wietz, M., Brinkhoff, T., Hehemann, J.-H., Probandt, D., Zeugner, L., and Amann, R.: The Biogeochemistry of Marine Polysaccharides: Sources, Inventories, and Bacterial Drivers of the Carbohydrate Cycle, Annu. Rev. Mar. Sci., 13, 81–108, https://doi.org/10.1146/annurev-marine-032020-012810, 2021.

Ascani, F., Richards, K. J., Firing, E., Grant, S., Johnson, K. S., Jia, Y., Lukas, R., and Karl, D. M.: Physical and biological controls of nitrate concentrations in the upper subtropical North Pacific Ocean, Deep Sea Res. Part II Top. Stud. Oceanogr., 93, 119–134, https://doi.org/10.1016/j.dsr2.2013.01.034, 2013.

Azetsu-Scott, K. and Passow, U.: Ascending marine particles: Significance of transparent exopolymer particles (TEP) in the upper ocean, Limnol. Oceanogr., 49, 741–748, https://doi.org/10.4319/lo.2004.49.3.0741, 2004.

Bar-Zeev, E., Berman, T., Rahav, E., Dishon, G., Herut, B., Kress, N., and Berman-Frank, I.: Transparent exopolymer particle (TEP) dynamics in the eastern Mediterranean Sea, Mar. Ecol. Prog. Ser., 431, 107–118, https://doi.org/10.3354/meps09110, 2011.

Beauvais, S., Pedrotti, M. L., Villa, E., and Lemée, R.: Transparent exopolymer particle (TEP) dynamics in relation to trophic and hydrological conditions in the NW Mediterranean Sea, Mar. Ecol. Prog. Ser., 262, 97–109, https://doi.org/10.3354/meps262097, 2003.

Berman-Frank, I., Rosenberg, G., Levitan, O., Haramaty, L., and Mari, X.: Coupling between autocatalytic cell death and transparent exopolymeric particle production in the marine cyanobacterium Trichodesmium, Environ. Microbiol., 9, 1415–1422, https://doi.org/10.1111/j.1462-2920.2007.01257.x, 2007.

Bhosle, N. B., Bhaskar, P. V., and Ramachandran, S.: Abundance of dissolved polysaccharides in the oxygen minimum layer of the Northern Indian Ocean, Mar. Chem., 63, 171–182, https://doi.org/10.1016/S0304-4203(98)00061-9, 1998.

Böttjer, D., Dore, J. E., Karl, D. M., Letelier, R. M., Mahaffey, C., Wilson, S. T., Zehr, J., and Church, M. J.: Temporal variability of nitrogen fixation and particulate nitrogen export at Station ALOHA, Limnol. Oceanogr., 62, 200–216, https://doi.org/10.1002/lno.10386, 2017.

Buesseler, K. O., Antia, A. N., Chen, M., Fowler, S. W., Gardner, W. D., Gustafsson, O., Harada, K., Michaels, A. F., Rutgers van der Loeff, M., Sarin, M., Steinberg, D. K., and Trull, T.: An assessment of the use of sediment traps for estimating upper ocean particle fluxes, J. Mar. Res., 65, 345–416, https://doi.org/10.1357/002224007781567621, 2007.

Burney, C. M., Johnson, K. M., Lavoie, D. M., and Sieburth, J. McN.: Dissolved carbohydrate and microbial ATP in the North Atlantic: concentrations and interactions, Deep Sea Res. Part Oceanogr. Res. Pap., 26, 1267–1290, https://doi.org/10.1016/0198-0149(79)90068-2, 1979.

747 Busch, K., Endres, S., Iversen, M. H., Michels, J., Nöthig, E.-M., and Engel, A.: Bacterial Colonization and
748 Vertical Distribution of Marine Gel Particles (TEP and CSP) in the Arctic Fram Strait, Front. Mar. Sci., 4,
749 2017.

750 Chin, W.-C., Orellana, M. V., and Verdugo, P.: Spontaneous assembly of marine dissolved organic matter
751 into polymer gels, Nature, 391, 568–572, https://doi.org/10.1038/35345, 1998.

752 Chow, C. H., Cheah, W., and Tai, J.-H.: A rare and extensive summer bloom enhanced by ocean eddies in
753 the oligotrophic western North Pacific Subtropical Gyre, Sci. Rep., 7, 6199,
754 https://doi.org/10.1038/s41598-017-06584-3, 2017.

755 Cisternas-Novoa, C., Lee, C., and Engel, A.: Transparent exopolymer particles (TEP) and Coomassie
756 stainable particles (CSP): Differences between their origin and vertical distributions in the ocean, Mar.
757 Chem., 175, 56–71, https://doi.org/10.1016/j.marchem.2015.03.009, 2015.

758 Dall'Olmo, G., Dingle, J., Polimene, L., Brewin, R. J., & Claustre, H. (2016). Substantial energy input to the
759 mesopelagic ecosystem from the seasonal mixed-layer pump. *Nature Geoscience*, *9*(11), 820-823.

760 Dave, A. C. and Lozier, M. S.: Local stratification control of marine productivity in the subtropical North
761 Pacific, J. Geophys. Res. Oceans, 115, https://doi.org/10.1029/2010JC006507, 2010.

762 Emerson, S.: Annual net community production and the biological carbon flux in the ocean, Glob.
763 Biogeochem. Cycles, 28, 14–28, https://doi.org/10.1002/2013GB004680, 2014.

764 Emerson, S. and Hayward, T.: Chemical tracers of biological processes in shallow waters of North Pacific:
765 preformed nitrate distributions., J. Mar. Res., 53, 499–513, 1995.

766 Emerson, S., Quay, P., Karl, D., Winn, C., Tupas, L., and Landry, M.: Experimental determination of the
767 organic carbon flux from open-ocean surface waters, Nature, 389, 951–954,
768 https://doi.org/10.1038/40111, 1997.

769 Engel, A. and Passow, U.: Carbon and nitrogen content of transparent exopolymer particles (TEP) in
770 relation to their Alcian Blue adsorption, Mar. Ecol. Prog. Ser., 219, 1–10,
771 https://doi.org/10.3354/meps219001, 2001.

772 Engel, A., Borchard, C., Loginova, A., Meyer, J., Hauss, H., and Kiko, R.: Effects of varied nitrate and
773 phosphate supply on polysaccharidic and proteinaceous gel particle production during tropical
774 phytoplankton bloom experiments, Biogeosciences, 12, 5647–5665, https://doi.org/10.5194/bg-12-
775 5647-2015, 2015.

776 Engel, A., Endres, S., Galgani, L., and Schartau, M.: Marvelous Marine Microgels: On the Distribution and
777 Impact of Gel-Like Particles in the Oceanic Water-Column, Front. Mar. Sci., 7,
778 https://doi.org/10.3389/fmars.2020.00405, 2020.

779 Fawcett, S. E., Johnson, K. S., Riser, S. C., Van Oostende, N., and Sigman, D. M.: Low-nutrient organic
780 matter in the Sargasso Sea thermocline: A hypothesis for its role, identity, and carbon cycle implications,
781 Mar. Chem., 207, 108–123, https://doi.org/10.1016/j.marchem.2018.10.008, 2018.

Goldberg, S. J., Carlson, C. A., Bock, B., Nelson, N. B., and Siegel, D. A.: Meridional variability in dissolved organic matter stocks and diagenetic state within the euphotic and mesopelagic zone of the North Atlantic subtropical gyre, Mar. Chem., 119, 9–21, https://doi.org/10.1016/j.marchem.2009.12.002, 2010.

Grossart, H.-P., Czub, G., and Simon, M.: Algae–bacteria interactions and their effects on aggregation and organic matter flux in the sea, Environ. Microbiol., 8, 1074–1084, https://doi.org/10.1111/j.1462-2920.2006.00999.x, 2006.

Gruber, N., Keeling, C. D., and Stocker, T. F.: Carbon-13 constraints on the seasonal inorganic carbon budget at the BATS site in the northwestern Sargasso Sea, Deep Sea Res. Part Oceanogr. Res. Pap., 45, 673–717, https://doi.org/10.1016/S0967-0637(97)00098-8, 1998.

Guo, S., Wu, Y., Zhu, M., and Sun, X.: Concentrations of transparent exopolymer particles (TEPs) and their role in the carbon export in the South China Sea and western tropical North Pacific, Mar. Environ. Res., 179, 105699, https://doi.org/10.1016/j.marenvres.2022.105699, 2022.

Hannides, C. C. S., Popp, B. N., Landry, M. R., and Graham, B. S.: Quantification of zooplankton trophic position in the North Pacific Subtropical Gyre using stable nitrogen isotopes, Limnol. Oceanogr., 54, 50–61, https://doi.org/10.4319/lo.2009.54.1.0050, 2009.

Hansell, D. A., & Carlson, C. A. (2001). Biogeochemistry of total organic carbon and nitrogen in the Sargasso Sea: control by convective overturn. *Deep Sea Research Part II: Topical Studies in Oceanography*, *48*(8-9), 1649-1667.

Hansell, D. A., Carlson, C. A., Repeta, D. J., & Schlitzer, R. (2009). Dissolved organic matter in the ocean: A controversy stimulates new insights. *Oceanography*, *22*(4), 202-211.

Iuculano, F., Mazuecos, I. P., Reche, I., and Agustí, S.: Prochlorococcus as a Possible Source for Transparent Exopolymer Particles (TEP), Front. Microbiol., 8, 2017.

von Jackowski, A., Grosse, J., Nöthig, E.-M., and Engel, A.: Dynamics of organic matter and bacterial activity in the Fram Strait during summer and autumn, Philos. Trans. R. Soc. Math. Phys. Eng. Sci., 378, 20190366, https://doi.org/10.1098/rsta.2019.0366, 2020.

Johnson, K. S., Riser, S. C., and Karl, D. M.: Nitrate supply from deep to near-surface waters of the North Pacific subtropical gyre, Nature, 465, 1062–1065, https://doi.org/10.1038/nature09170, 2010.

Kaiser, K. and Benner, R.: Organic matter transformations in the upper mesopelagic zone of the North Pacific: Chemical composition and linkages to microbial community structure, J. Geophys. Res. Oceans, 117, https://doi.org/10.1029/2011JC007141, 2012.

Karl, D. M., Church, M. J., Dore, J. E., Letelier, R. M., and Mahaffey, C.: Predictable and efficient carbon sequestration in the North Pacific Ocean supported by symbiotic nitrogen fixation, Proc. Natl. Acad. Sci., 109, 1842–1849, https://doi.org/10.1073/pnas.1120312109, 2012.

Karl, D. M., Letelier, R. M., Bidigare, R. R., Björkman, K. M., Church, M. J., Dore, J. E., and White, A. E.: Seasonal-to-decadal scale variability in primary production and particulate matter export at Station ALOHA, Prog. Oceanogr., 195, 102563, https://doi.org/10.1016/j.pocean.2021.102563, 2021.

819 Keeling, C. D., Brix, H., and Gruber, N.: Seasonal and long-term dynamics of the upper ocean carbon
820 cycle at Station ALOHA near Hawaii, Glob. Biogeochem. Cycles, 18,
821 https://doi.org/10.1029/2004GB002227, 2004.

822 Lamborg, C. H., Buesseler, K. O., Valdes, J., Bertrand, C. H., Bidigare, R., Manganini, S., Pike, S., Steinberg,
823 D., Trull, T., and Wilson, S.: The flux of bio- and lithogenic material associated with sinking particles in
824 the mesopelagic "twilight zone" of the northwest and North Central Pacific Ocean, Deep Sea Res. Part II
825 Top. Stud. Oceanogr., 55, 1540–1563, https://doi.org/10.1016/j.dsr2.2008.04.011, 2008.

826 Letelier, R. M., Björkman, K. M., Church, M. J., Hamilton, D. S., Mahowald, N. M., Scanza, R. A.,
827 Schneider, N., White, A. E., and Karl, D. M.: Climate-driven oscillation of phosphorus and iron limitation
828 in the North Pacific Subtropical Gyre, Proc. Natl. Acad. Sci., 116, 12720–12728,
829 https://doi.org/10.1073/pnas.1900789116, 2019.

830 Letscher, R. T. and Villareal, T. A.: Evaluation of the seasonal formation of subsurface negative
831 preformed nitrate anomalies in the subtropical North Pacific and North Atlantic, Biogeosciences, 15,
832 6461–6480, https://doi.org/10.5194/bg-15-6461-2018, 2018.

833 Liang, Z., Letscher, R. T., and Knapp, A. N.: Global patterns of surface ocean dissolved organic matter
834 stoichiometry, *Global Biogeochemical Cycles*, 37(12), e2023GB007788,
835 https://doi.org/10.1029/2023GB007788, 2023.

836 Ling, S. C. and Alldredge, A. L.: Does the marine copepod Calanus pacificus consume transparent
837 exopolymer particles (TEP)?, J. Plankton Res., 25, 507–515, https://doi.org/10.1093/plankt/25.5.507,
838 2003.

839 Long, J., Fassbender, A., and Estapa, M.: Depth-Resolved Net Primary Production in the Northeast Pacific
840 Ocean: A Comparison of Satellite and Profiling Float Estimates in the Context of Two Marine Heatwaves,
841 Geophys. Res. Lett., 48, https://doi.org/10.1029/2021GL093462, 2021.

842 Longhurst, A., Sathyendranath, S., Platt, T., and Caverhill, C.: An estimate of global primary production in
843 the ocean from satellite radiometer data, J. Plankton Res., 17, 1245–1271,
844 https://doi.org/10.1093/plankt/17.6.1245, 1995.

845 Mari, X., Beauvais, S., Lemée, R., and Pedrotti, M. L.: Non-Redfield C:N ratio of transparent exopolymeric
846 particles in the northwestern Mediterranean Sea, Limnol. Oceanogr., 46, 1831–1836,
847 https://doi.org/10.4319/lo.2001.46.7.1831, 2001.

848 Mari, X., Rochelle-Newall, E., Torréton, J.-P., Pringault, O., Jouon, A., and Migon, C.: Water residence
849 time: A regulatory factor of the DOM to POM transfer efficiency, Limnol. Oceanogr., 52, 808–819,
850 https://doi.org/10.4319/lo.2007.52.2.0808, 2007.

851 Mari, X., Passow, U., Migon, C., Burd, A. B., and Legendre, L.: Transparent exopolymer particles: Effects
852 on carbon cycling in the ocean, Prog. Oceanogr., 151, 13–37,
853 https://doi.org/10.1016/j.pocean.2016.11.002, 2017.

854 McCarthy, M., Hedges, J., and Benner, R.: Major biochemical composition of dissolved high molecular
855 weight organic matter in seawater, Mar. Chem., 55, 281–297, https://doi.org/10.1016/S0304-
856 4203(96)00041-2, 1996.

Meers, E., Laing, G. D., Unamuno, V. G., Lesage, E., Tack, F. M. G., and Verloo, M. G.: Water Extractability of Trace Metals from Soils: Some Pitfalls, Water. Air. Soil Pollut., 176, 21–35, https://doi.org/10.1007/s11270-005-9070-1, 2006.

Michaels, A. F., Bates, N. R., Buesseler, K. O., Carlson, C. A., and Knap, A. H.: Carbon-cycle imbalances in the Sargasso Sea, Nature, 372, 537–540, https://doi.org/10.1038/372537a0, 1994.

Nagata, T., Yamada, Y., and Fukuda, H.: Transparent Exopolymer Particles in Deep Oceans: Synthesis and Future Challenges, Gels, 7, 75, https://doi.org/10.3390/gels7030075, 2021.

Nosaka, Y., Yamashita, Y., and Suzuki, K.: Dynamics and Origin of Transparent Exopolymer Particles in the Oyashio Region of the Western Subarctic Pacific during the Spring Diatom Bloom, Front. Mar. Sci., 4, 2017.

Ortega-Retuerta, E., Passow, U., Duarte, C. M., and Reche, I.: Effects of ultraviolet B radiation on (not so) transparent exopolymer particles, Biogeosciences, 6, 3071–3080, https://doi.org/10.5194/bg-6-3071-2009, 2009a.

Ortega-Retuerta, E., Reche, I., Pulido-Villena, E., Agustí, S., and Duarte, C. M.: Uncoupled distributions of transparent exopolymer particles (TEP) and dissolved carbohydrates in the Southern Ocean, Mar. Chem., 115, 59–65, https://doi.org/10.1016/j.marchem.2009.06.004, 2009b.

Ortega-Retuerta, E., Mazuecos, I. P., Reche, I., Gasol, J. M., Álvarez-Salgado, X. A., Álvarez, M., Montero, M. F., and Arístegui, J.: Transparent exopolymer particle (TEP) distribution and in situ prokaryotic generation across the deep Mediterranean Sea and nearby North East Atlantic Ocean, Prog. Oceanogr., 173, 180–191, https://doi.org/10.1016/j.pocean.2019.03.002, 2019.

Pakulski, J. D. and Benner, R.: Abundance and distribution of carbohydrates in the ocean, Limnol. Oceanogr., 39, 930–940, https://doi.org/10.4319/lo.1994.39.4.0930, 1994.

Passow, U.: Formation of transparent exopolymer particles, TEP, from dissolved precursor material, Mar. Ecol. Prog. Ser., 192, 1–11, https://doi.org/10.3354/meps192001, 2000.

Passow, U.: Production of transparent exopolymer particles (TEP) by phyto- and bacterioplankton, Mar. Ecol. Prog. Ser., 236, 1–12, https://doi.org/10.3354/meps236001, 2002a.

Passow, U.: Transparent exopolymer particles (TEP) in aquatic environments, Prog. Oceanogr., 55, 287–333, https://doi.org/10.1016/S0079-6611(02)00138-6, 2002b.

Passow, U., Alldredge, A. L., and Logan, B. E.: The role of particulate carbohydrate exudates in the flocculation of diatom blooms, Deep Sea Res. Part Oceanogr. Res. Pap., 41, 335–357, https://doi.org/10.1016/0967-0637(94)90007-8, 1994.

Pilskaln, C. H., Villareal, T. A., Dennett, M., Darkangelo-Wood, C., and Meadows, G.: High concentrations of marine snow and diatom algal mats in the North Pacific Subtropical Gyre: Implications for carbon and nitrogen cycles in the oligotrophic ocean, Deep Sea Res. Part Oceanogr. Res. Pap., 52, 2315–2332, https://doi.org/10.1016/j.dsr.2005.08.004, 2005.

van Pinxteren, M., Robinson, T.-B., Zeppenfeld, S., Gong, X., Bahlmann, E., Fomba, K. W., Triesch, N., Stratmann, F., Wurl, O., Engel, A., Wex, H., and Herrmann, H.: High number concentrations of transparent exopolymer particles in ambient aerosol particles and cloud water – a case study at the tropical Atlantic Ocean, Atmospheric Chem. Phys., 22, 5725–5742, https://doi.org/10.5194/acp-22-5725-2022, 2022.

Prairie, J. C., Montgomery, Q. W., Proctor, K. W., and Ghiorso, K. S.: Effects of Phytoplankton Growth Phase on Settling Properties of Marine Aggregates, J. Mar. Sci. Eng., 7, 265, https://doi.org/10.3390/jmse7080265, 2019.

Quay, P., Emerson, S., and Palevsky, H.: Regional Pattern of the Ocean's Biological Pump Based on Geochemical Observations, Geophys. Res. Lett., 47, e2020GL088098, https://doi.org/10.1029/2020GL088098, 2020.

Quay, P., & Stephens, M. (2025). Regional patterns of organic matter export rates along the GEOTRACES Pacific meridional transect GP15. *Global Biogeochemical Cycles*, *39*(2), e2024GB008277.

Quigg, A., Santschi, P. H., Burd, A., Chin, W. C., Kamalanathan, M., Xu, C., & Ziervogel, K. (2021). From nano-gels to marine snow: A synthesis of gel formation processes and modeling efforts involved with particle flux in the ocean. *Gels*, *7*(3), 114.

Rabouille, S., Cabral, G. S., and Pedrotti, M. L.: Towards a carbon budget of the diazotrophic cyanobacterium Crocosphaera: effect of irradiance, Mar. Ecol. Prog. Ser., 570, 29–40, https://doi.org/10.3354/meps12087, 2017.

Radić, T., Ivančić, I., Fuks, D., and Radić, J.: Marine bacterioplankton production of polysaccharidic and proteinaceous particles under different nutrient regimes, FEMS Microbiol. Ecol., 58, 333–342, https://doi.org/10.1111/j.1574-6941.2006.00176.x, 2006.

Reygondeau, G., Longhurst, A., Martinez, E., Beaugrand, G., Antoine, D., and Maury, O.: Dynamic biogeochemical provinces in the global ocean, Glob. Biogeochem. Cycles, 27, 1046–1058, https://doi.org/10.1002/gbc.20089, 2013.

Rochelle-Newall, E. J., Mari, X., and Pringault, O.: Sticking properties of transparent exopolymeric particles (TEP) during aging and biodegradation, J. Plankton Res., 32, 1433–1442, https://doi.org/10.1093/plankt/fbq060, 2010.

Roshan, S. and DeVries, T.: Efficient dissolved organic carbon production and export in the oligotrophic ocean, Nat. Commun., 8, 2036, https://doi.org/10.1038/s41467-017-02227-3, 2017.

Sambrotto, R. N., Savidge, G., Robinson, C., Boyd, P., Takahashi, T., Karl, D. M., Langdon, C., Chipman, D., Marra, J., and Codispoti, L.: Elevated consumption of carbon relative to nitrogen in the surface ocean, Nature, 363, 248–250, https://doi.org/10.1038/363248a0, 1993.

Smith, D. C., Simon, M., Alldredge, A. L., and Azam, F.: Intense hydrolytic enzyme activity on marine aggregates and implications for rapid particle dissolution, Nature, 359, 139–142, https://doi.org/10.1038/359139a0, 1992.

928 Smyth, A. J., and Letscher, R. T.: Spatial and temporal occurrence of preformed nitrate anomalies in the
929 subtropical North Pacific and North Atlantic oceans, *Marine Chemistry*, *252*, 104248,
930 https://doi.org/10.5194/bg-15-6461-2018, 2023.

931 Sun, C.-C., Sperling, M., and Engel, A.: Effect of wind speed on the size distribution of gel particles in the
932 sea surface microlayer: insights from a wind–wave channel experiment, Biogeosciences, 15, 3577–3589,
933 https://doi.org/10.5194/bg-15-3577-2018, 2018.

934 Teng, Y.-C., Primeau, F. W., Moore, J. K., Lomas, M. W., and Martiny, A. C.: Global-scale variations of the
935 ratios of carbon to phosphorus in exported marine organic matter, Nat. Geosci., 7, 895–898,
936 https://doi.org/10.1038/ngeo2303, 2014.

937 Thompson, A. W., van den Engh, G., Ahlgren, N. A., Kouba, K., Ward, S., Wilson, S. T., and Karl, D. M.:
938 Dynamics of Prochlorococcus Diversity and Photoacclimation During Short-Term Shifts in Water Column
939 Stratification at Station ALOHA, Front. Mar. Sci., 5, 2018.

940 Thornton, D. C. O.: Coomassie Stainable Particles (CSP): Protein Containing Exopolymer Particles in the
941 Ocean, Front. Mar. Sci., 5, 2018.

942 Toggweiler, J. R.: Carbon overconsumption, Nature, 363, 210–211, https://doi.org/10.1038/363210a0,
943 1993.

944 Verdugo, P.: Marine microgels, Annual Review of Marine Science, 4(1), 375-400, 2012.

945 Verdugo, P., Alldredge, A. L., Azam, F., Kirchman, D. L., Passow, U., & Santschi, P. H.: The oceanic gel
946 phase: a bridge in the DOM–POM continuum. Marine chemistry, 92(1-4), 67-85, 2004.

947 Villareal, T. A., Pilskaln, C. H., Montoya, J. P., and Dennett, M.: Upward nitrate transport by
948 phytoplankton in oceanic waters: balancing nutrient budgets in oligotrophic seas, PeerJ, 2, e302,
949 https://doi.org/10.7717/peerj.302, 2014.

950 Westberry, T. K., Silsbe, G. M., and Behrenfeld, M. J.: Gross and net primary production in the global
951 ocean: An ocean color remote sensing perspective, Earth-Sci. Rev., 237, 104322,
952 https://doi.org/10.1016/j.earscirev.2023.104322, 2023.

953 Williams, P. J. le B., Quay, P. D., Westberry, T. K., and Behrenfeld, M. J.: The Oligotrophic Ocean Is
954 Autotrophic, Annu. Rev. Mar. Sci., 5, 535–549, https://doi.org/10.1146/annurev-marine-121211-172335,
955 2013.

956 Wurl, O., Wurl, E., Miller, L., Johnson, K., and Vagle, S.: Formation and global distribution of sea-surface
957 microlayers, Biogeosciences, 8, 121–135, https://doi.org/10.5194/bg-8-121-2011, 2011a.

958 Wurl, O., Miller, L., and Vagle, S.: Production and fate of transparent exopolymer particles in the ocean,
959 J. Geophys. Res. Oceans, 116, https://doi.org/10.1029/2011JC007342, 2011b.

960 Zamanillo, M., Ortega-Retuerta, E., Nunes, S., Estrada, M., Sala, M. M., Royer, S.-J., López-Sandoval, D.
961 C., Emelianov, M., Vaqué, D., Marrasé, C., and Simó, R.: Distribution of transparent exopolymer particles
962 (TEP) in distinct regions of the Southern Ocean, Sci. Total Environ., 691, 736–748,
963 https://doi.org/10.1016/j.scitotenv.2019.06.524, 2019.

964 Zamanillo, M., Ortega-Retuerta, E., Cisternas-Novoa, C., Marrasé, C., Pelejero, C., Pascual, J., Gasol, J. M.,
965 Engel, A., and Simó, R.: Uncoupled seasonal variability of transparent exopolymer and Coomassie
966 stainable particles in coastal Mediterranean waters: Insights into sources and driving mechanisms, Elem.
967 Sci. Anthr., 9, 00165, https://doi.org/10.1525/elementa.2020.00165, 2021.

968 Zäncker, B., Bracher, A., Röttgers, R., and Engel, A.: Variations of the Organic Matter Composition in the
969 Sea Surface Microlayer: A Comparison between Open Ocean, Coastal, and Upwelling Sites Off the
970 Peruvian Coast, Front. Microbiol., 8, 2017.

971

972